www.editada.org

International Journal of Combinatorial Optimization Problems and Informatics, 11(1), Jan-April 2020, 59-75. ISSN: 2007-1558.

Reduction of the Fused Filament Fabrication Process Time in the Manufacturing of Printed Circuit Board Slots

Julian I. Aguilar-Duque[1,2], Juan L. Hernández-Arellano[2], Cesar O. Balderrama-Armendariz[2], Liliana Avelar-Sosa[2]
[1] Universidad Autonóma de Baja California
[2] Universidad Autonóma de Ciudad Juárez
julian.aguilar@uabc.edu.mx, al171870@alumnos.uacj.mx

Abstract. Fused Filament Fabrication is an Additive Manufacturing technology that is continuously improving its technologies. The present research exposes the use of the Travel Salesman Problem and Nearest Neighbor Algorithm as a strategy to reduce the time need to print slots shield in a Printed Circuit Board. The methodology used describes the process from the design to the printing board. A board of 98 slots of four geometries was analyzed. The results present a reduction of 5.88% of the original time required to print the board.

Keywords: Fused Filament Fabrication, Travel Salesman Problem, Nearest Neighbor Algorithm, time reduction process, PCB board.

Article Info
Received Sep 26, 2018
Accepted Sep 11, 2019

1 Introduction

Manufacturing systems have evolved from the appearance of the first stone tools to the new automatized era. In this sense, it is possible to ensure that the actual manufacturing is the result of continuous improvement of machinery, human factors, materials, and also the methods used to produce goods or services. The evolution of the elements mentioned can be summarized in four groups. First, the development of machinery and equipment were focused in the creation of new technologies to facilitate processes, increase productivity, and ensure the physical integrity of the human resource involved in the process, all of them were affected by the use of electronics, semi-automatized, and automatized equipment [1]. Second, the human factor has been forced to evolve along with technology, making evident the demand of a human factor with new abilities (handle of digital equipment), and knowledge focused in the operation of sophisticated equipment, involved with the task and also committed to continuous improvement [2, 3]. Third, innovative materials that allow the creation of products that improve the quality of humans life, that are friendly with the environment, and also are self-sustaining [4]. Finally, the methods used to achieve the goals, which are focused on improving the resources involved in the manufacturing system [5]. All of them with a concept in common “Optimization.” This means that their evolution is continuous and have been producing favorable results, that have been increasing until 80% the capacity of produce goods if we compare the 80’s with the new era [6].

1.1 Background

Before 1980, the world of manufacture was immersed in subtractive processes of raw material. With the advent of Additive Manufacturing (AM) in the early ’80s, the paradigms of traditional manufacturing systems were broken arisen the develop of new fabrication technologies and more efficient processes from the point of view of savings materials [7-9]. Then, AM was considered the complement of Subtractive Manufacturing (SM), and it has evolved to have the seven technologies that define it today. These technologies are: 1) Stereolithography (SLA), 2) Laminated Object Manufacturing (LOM), 3) 3D printing (3DP), 4) Selective Laser Sintering (SLS), 5) Laser Engineered Net Shaping (LENS), 6) Electron Beam Melting, and 7) Fused Deposition Modeling or Fused Filament Fabrication[8-12]. The description and function of these technologies are synthesized and present in Figure 1.

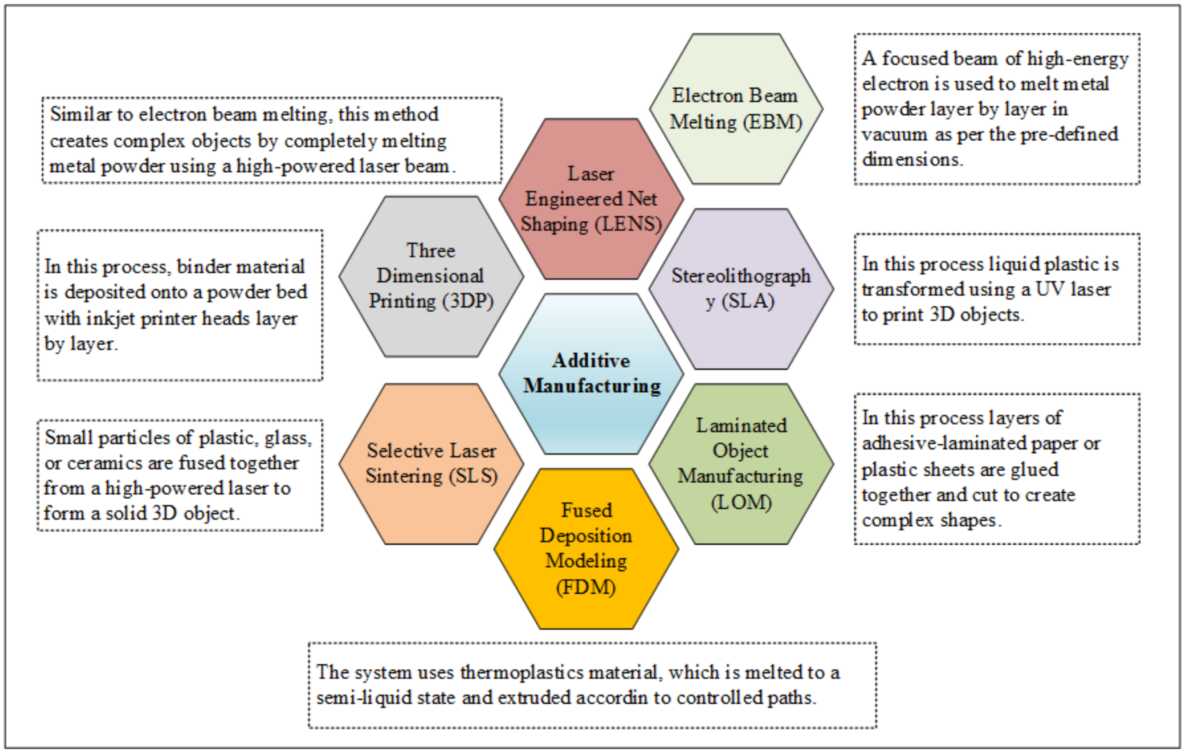

Fig. 1. Additive Manufacturing Technologies.

Even the process of the seven AM technologies is similar (addition of material by layers), the real difference is the equipment used and the form of the material (liquid, wire, powder or sheets). Generally, the process is classified in three stages; stage one “pre-process” [13–15], stage two “process” [12, 13, 16–18] and, stage three post-process [16, 17].

The pre-processing starts with the conceptualization and design. These activities are developed using computers and specific design software as a Computer Aided Design (CAD) or Computer Aided Engineering (CAE). Once the design has been defined, it is necessary to transform the design in a series of operating instructions that AM equipment can interpret to execute and materialize the design. To create a file with the instruction, the designer should save the design in a Standard Triangle Language (.stl) first. Then, load the stl file in AM software to prepare the design for the AM process. The preparation consists in to define the parameters of the equipment as well as the material and the orientation of the object to create a G-code. Due that this stage involves strategies of programing language; it is possible to develop improvements in the instruction code, focused on optimizing the equipment performance.

The second stage or process is done using any of the seven AM technologies. The selection of the AM technology depends on the function for which the object was designed in stage one. The use of materials as metals, polymers, and resins as well as the form of the material as wire, liquid, granulates, or powder is linked with the AM technology used to print the component. For example, if the customer needs a component in steel alloy, the best alternative of AM technology is Electron Beam Melting (EBM) which uses steel powder. In case of the customer needs a flexible component as a shoe sole, the best option is Fused Filament Fabrication AM technology with a flexible filament. Process stage ends when the AM equipment finishes the printing process; in this stage, it is possible that the component has imperfections or defects that can be repaired using post-processing activities.

Lastly, the third stage or post-process integrates manufacturing activities to finish the element such as cutting, polishing, and packing. Many companies around the world supply equipment and services of AM post-processing as a reduction of roughness for FDM, SLS, SLA, among others. Painting process using electrostatic process or steam bath acetone for some plastics. It is essential to highlight that in industrial environments; the post-process activities also include quality assurance and post sales services. To synthesize the stages described, Figure 2 is used to resume the general flow of activities in a typical AM process.

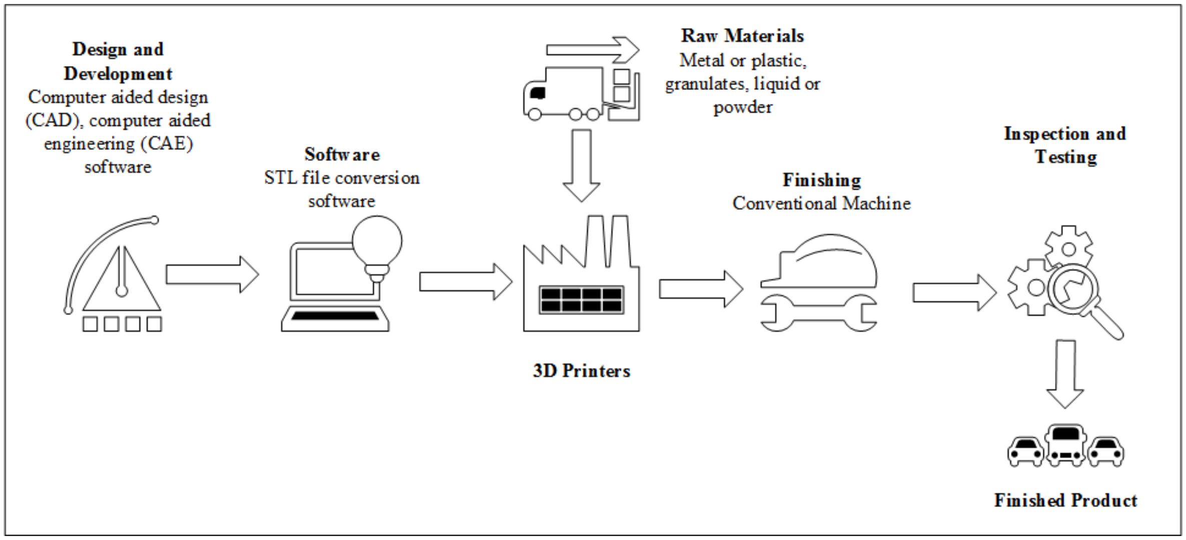

Fig. 2. General Flow Chart of Additive Manufacturing activities.

Since its creation until now, AM has been evolved in different ways. This evolution made it possible to differentiate each technology, considering their strengths and weaknesses. [21,22], describes the advantages and disadvantages of AM technologies synthesized in Table 1.

Table 1. Advantages and disadvantages of AM technologies [21,22]

Technology	Advantages	Disadvantages
Stereolithography	Suitable for production concept prototypes. Fast processing times and good surface finish and geometrical accuracy.	Limited to process no-functional materials such as resins or plastics. Resins are cost-expensive and limited in availability. Unable to process functional material such as metals. Requires support structures, among others.
Selective Laser Sintering	Materials which can be processed include plastics, ceramics, sands and some metals. Parts produced are suitable for functional testing, and No support structures are required during processing.	Availability of metallic materials is narrow. An enclosed chamber is required, and metal sintering leads to porous and mechanically weak components.
Selective Laser Melting	Good geometrical accuracy. No support structures are required. Suitable for the processing of metallic materials and Produced components are near fully-dense, suitable for functional use.	Size of produced components is limited by dimensions of enclosing chamber, Availability of materials is limited. Slow build-up rate and machining may be required for accurate dimensioning and improving surface finish.
Laminated Object Manufacturing	Suitable for processing of medium and large sized components, such as dies or metal forming tools and a wide choice of readily available materials in sheet form.	Poor layer bonding carries the risk of de-lamination. Strength of the produced components in the perpendicular direction to the layers is much less than in other directions, and various post-processing are required.

3-D printing	High productivity. Good geometrical accuracy and no support structures are required.	Time-consuming post-processing operations are required. Furnace heating is required to eliminate the binder. The sintered part is porous. Mechanical strength of produced components is low and limited choice of materials.
Direct Metal Deposition	The layer can be fabricated in any orientation; a variety of materials in powder form can be processed. Large components can be manufactured, and Higher deposition rates are possible.	Geometrical accuracy is lower. The stair-stepping effect can limit geometrical accuracy, and post-processing operations may be required.
Fused Deposition Modeling (FDM) or Fuse Filament Fabrication (FFF)	Is the most popular technology to create products. Lower cost is the cheapest AM technology. The broad range in materials. Almost no post-processing is need; the product is quickly ready for use. More accessible than the other AM technologies.	Cannot deliver a high-quality product. Restricted range of materials. For extra fine features requires special finishing products.

As described in Table 1, FFF is the most popular AM technology because of its advantages compared to other AM technologies. It is important to highlight that FFF presents a growth of 23.25% that involves printer, material, software, service, process, application, and technology. Although, the most important reason for FFF success, should focus on its capacity to print components in a faster and more effective way [23].

Due to its nature, AM is in a disadvantage against SM from production capacity [12, 16, 17]. During the last thirty years of research in AM, the efforts had been focused on improving the performance of equipment [20–22], mainly in modifications of solidification and injection of material, development of cabins for the control of the environment, reduction in the structural variability of the components, among others. One of the most significate advances in the research field of AM is the development of software and controllers which are similar in principle to those used in SM. These advances have opened the opportunity to use optimization algorithms that were successful in SM and can be adopted in AM.

One of the pioneer industries in AM has been the electronic manufacturers, who have faced the demand for variable volumes of production in specific components. One of this component is the board used in the manufacture of Printed Circuit Board (PCB) (see an example of PCB in Figure 3). An important characteristic that restricts the productivity of PCB’s is the drilling operation on the boards for PCB, which is entirely absorbable when manufacturers use SM in batches larger than 5,000 units. The problem is when the production demand of board is smaller of 1,000 units, under this demand, SM increase the manufacturer cost of the board up to 400% [24, 25]. To solve this problem, some researches have been focused in the optimization of the drilling process with positive results in a high volume of production [25–27], although these strategies have not been successful in low production batches using SM.

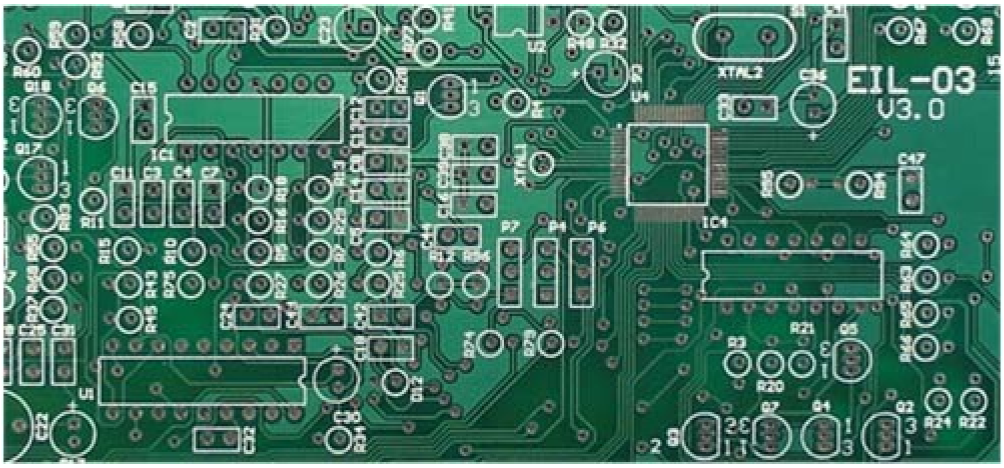

Fig. 3. Part of a PCB of two layers [32].

1.2 Objective

The present research aims to expose the reduction in the time of the production process of the board for PCB using the technology of Fused Filament Fabrication (FFF). Because the path of the extruder represents a problem that can be represented by the Traveling Salesman Problem, the Nearest Neighbor Algorithm was selected to determine the smallest printing route required to print the board.

2 Heuristic optimization algorithms

The study of optimization techniques has evolved from the development of exact algorithms to heuristics and metaheuristics. This evolution has generated positive results when the solution approach is directed towards the number of existing routes, the identification of possible solutions, and the appropriate path [33]. There are two reasons to use heuristic methods to the solution of optimization problems: 1) because it does not exist an exact algorithm with polynomial complexity that finds the optimal solution, and 2) the cardinality of search space for these problems is usually very large, which makes the use of exact algorithms unfeasible since the amount of time it takes to find the solution is unacceptable.

Classification for the heuristic methods [33].

- Constructive methods. These methods build the solution from a strategy. The most common are; a) voracious strategy, b) decomposition strategy, c) reduction methods, and d) model manipulation methods.
- Search methods, which start from a feasible solution, and they try to improve it. Some of the most used are; a) local search strategy I, b) local search strategy II, and c) randomized strategy.

2.1 Travel Salesman Problem algorithm

There is much research focused on the development of algorithms that calculate the minimum route made by the resource (machine, transport, human, among others). However, the present research is focused in the calculation of the minimum path of the extruder that is covered during the formation of shields that function as a delimitation of the geometries using the Travel Salesman Problem algorithm (TSP). According to [34], TSP establishes that:

Given a matrix $C = \|c_{ij}\|$ (i=1,2,…,n, j=1,2,…,n) and the set of S of all possible sequences s of ordered pairs (i,j), for which

- All values for i=1,2,…,n and j=1,2,…,n occurs at least once in each s.
- If (i_1,j_1) and (i_2,j_2) are consecutive pars of s, then $j_1=i_2$
- If (i_1,j_1) is the first element and (i_m,j_m) is the last element of s, then $j_m=i_1$

The solution consists in found the sequence of $s_0 \in$ S, for which $M(s_o) = \min_s M(s)$ where the mean $M(s)$ is the sequence that is defined by $M(s) = \Sigma_{(i,j)}\, c_{ij}$, and the set of S can be represented by a) the set T of the sequence t integers, in which every integer between 1 and n occurs at least once in t, and b) by the set of de X of all the matrixes $X = \|x_{ij}\|$ that occur if $(i,j) \in s$, then $x_{ij}=1$ *and if (i,j)* $\not\subset$ *then* $x_{ij}=0$.

2.2 Nearest Neighbor Algorithm

Even there are different algorithms to solve the TSP; the present research uses the Nearest Neighbor Algorithm (NNA) due that the Fused Filament Fabrication process fits perfectly with K-NN. K-NN follows the next steps:

(1) Initialize all vertices as unvisited.
(2) Select an arbitrary vertex; set is as the current vertex *a*. Mark *a* as a visited.
(3) Find out the shortest edge connecting the current vertex *a* and an unvisited vertex *b*.
(4) Set *b* as the current vertex *a.* Mark *b* as visited.
(5) If all the vertices in the domain were visited, then terminate. Else, go to step 3.

The sequence of the visited vertices is the output of the algorithm. For this research, the algorithm was not used to classify the elements, was used to generate the sequence of initial coordinates based in the minimum distance. Is, for this reason, that k=1. According to [35], it is possible to weight the contribution of each neighbor considering the distance between neighbors x_q, giving high weigh to closest neighbors. In this case;

$$F(x_q) \leftarrow argmax_{v \epsilon V}\, \Sigma w_i \delta(v, f(x_i))$$

Where

$$w_i = 1 / d(x_q, x_i)^2$$

3 Experimental procedures

3.1 Materials

The present research uses the next materials and equipment:

- Personal computer.
- Software SolidWorks® [36] is the design software used to design the PCB.
- Software Cura® [37]. This software was used to prepare the component before the printing process, including in the preparation of process features of quality and resistance, as well as the printing machine parameters.
- Software Repetier® [38]. Repetier® was selected as software to generate the G-code. The G-code allows identifying the coordinates and the movements that the extruder should do to print the component.
- Software MATLAB® [39]. This research aims to analyze the times generated by the extruder during the printing process. In this case, MATLAB® was used to run the algorithm and obtain the routes as well as the time required to cover the route.
- TSP code generated by [40]. This program was used to evaluate the efficiency of routes generated by the nearest neighbor algorithm.
- Prusa I3® 3D printer. Once the route with the minimum printing time was defined, a 3D printing Prusa was used to print the component with the route modified. The PCB was produced using PLA Filament of 1.75 mm of diameter.

3.2 Method

Three phases integrated the method used to achieve the aim:

- Phase 1: “Board Design.” The board used for the analysis was developed considering the standards of the Association Connecting Electronics Industries (IPC) 2221B, and 2223D. For the design, SolidWorks 2018 software was used. The PBC designed is showed in Figure 5. This component has four square slots of 2.80 x 1.00 mm, six round slots of 0.70 mm of diameter, two round slots of 0.90 mm of diameter and 82 round slots of 0.45 mm. The slots are contained in an area of 38.48 x 44.07 x 0.5 mm. Once the design is complete, a .stl file is generated for the pre-processing.
- Phase 2: “pre-process.” To achieve this phase, the next activities were integrated.
  - Set the printing file using software Cura® 3.2.1 to define the orientation of the object and the parameters of the equipment. Using the .stl file generated in the design process, the object is loaded in the CURA® platform to define features of the material, the nozzle diameter, the printing speed, and the cooling speed. A .3mf file is generated with the information of the component.
  - G code: Once that the .3mf file is ready; software Repetier® is used to generate the G code that contains the coordinates that the equipment should follow at the moment of print the element. A .txt file is generated with the information of each coordinate; this file will be used in MATLAB® to run the optimization path algorithm.

- Path Optimization. The coordinates generated by Repetier® are used to create the values of the variables x and y, these values are used to define the path that the tool should follow to create the element. Using the K-NN algorithm programmed in MATLAB®, a group of solutions is generated, and the solutions present different scenarios that depend on the restrictions. Each solution proposes a sequence of points that are used to modify the G-code and create a new alternative of the printing process.

- Phase 3: "3D printing". In this phase, the component is printed. Before the printing, a set-up of the equipment is necessary. Prusa I3® equipment was selected. This phase aims to print the component, define the real printing time and the quality of the board.

Figure 4, exposes the scheme of the method used in this research, it is clear that phase one is focused on the design, phase two is used to prepare the component and optimize the time of PCB printing, and phase three is used to evaluate the features of the PCB and validate the times of printing process.

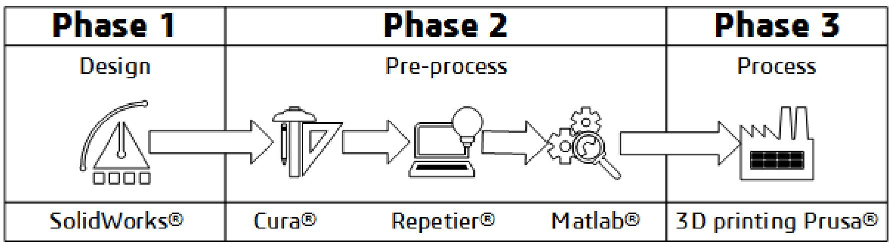

Fig. 4. Method of Optimization of the Fused Filament Fabrication Process in the Manufacturing of Printed Circuit Board.

4 Results

Figure 5 presents the design of the PCB board. The board has a thickness of 0.500 mm with a length of 44.070 mm and a width of 38.480 mm. The board has four types of slots. Four type A (rectangular) with dimensions of 1.000 x 2.800 mm. Six of type B (circular) with 0.700 mm of diameter. Two of type C (circular) with 0.450 mm of diameter, and 82 of type D (circular) with 0.450 mm of diameter.

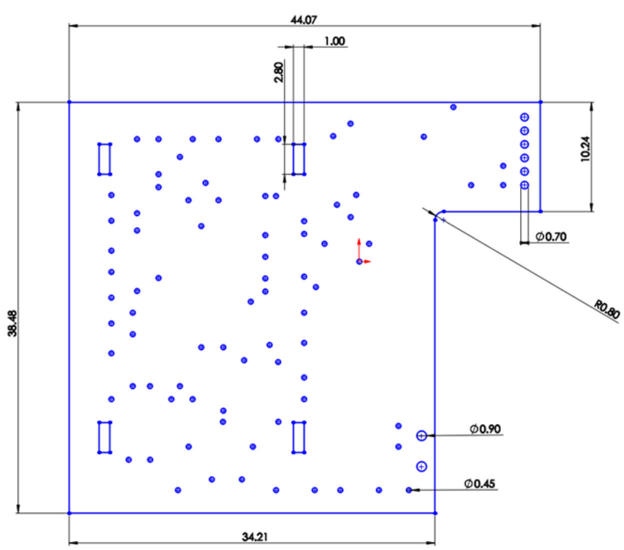

Fig. 5. Design of Board for PCB.

Once the board file was ready in pre-print, the next step was to simulate the printing process using Cura®. Before the simulation, the orientation of the object and the parameters of the equipment were defined. For the present research, polylactide PLA of 1.75 mm was used. The parameters defined for the Fused Filament Fabrication (FFF) were the next.

- Prusa I3 equipment. Format of 200 (200x200x200) mm, one extruder, diameter of the nozzle 0.200 mm.
- Quality: Layer Height 0.100 mm.
- Shell: Wall thickness 0.400 mm, Top/Bottom Thickness 0.800 mm.
- Infill: Density 90%, Infill pattern “grid”, gradual infill steps 5.
- Material: Printing temperature 200°C, build plate temperature 60°C, diameter 1.750 mm, flow 100%. Enable retraction.
- Speed: print speed 60 mm/s, travel speed 120 mm/s.
- Enable print cooling.
- Enable support.
- Build plate adhesion type: 8.000 mm border.

Cura® estimated that the time required for the printing was of 17 minutes, with a consumption of 0.48 meters of PLA. The board requires the printing of four layers. Figure 6.a present the route of the tool to print layer 1. Figure 6.b exposes the route of the tool to create layer 2. Figure 6.c present the routes that the tool should cover to create layer 3, and finally, Figure 6.d presents layer 4. The orientation of the element whit x-y elements, do not represent significate changes in the time required for the board fabrication. As a consequence, the lateral face of 44.070 millimeters of the board was oriented in parallel with the X plate printing axis.

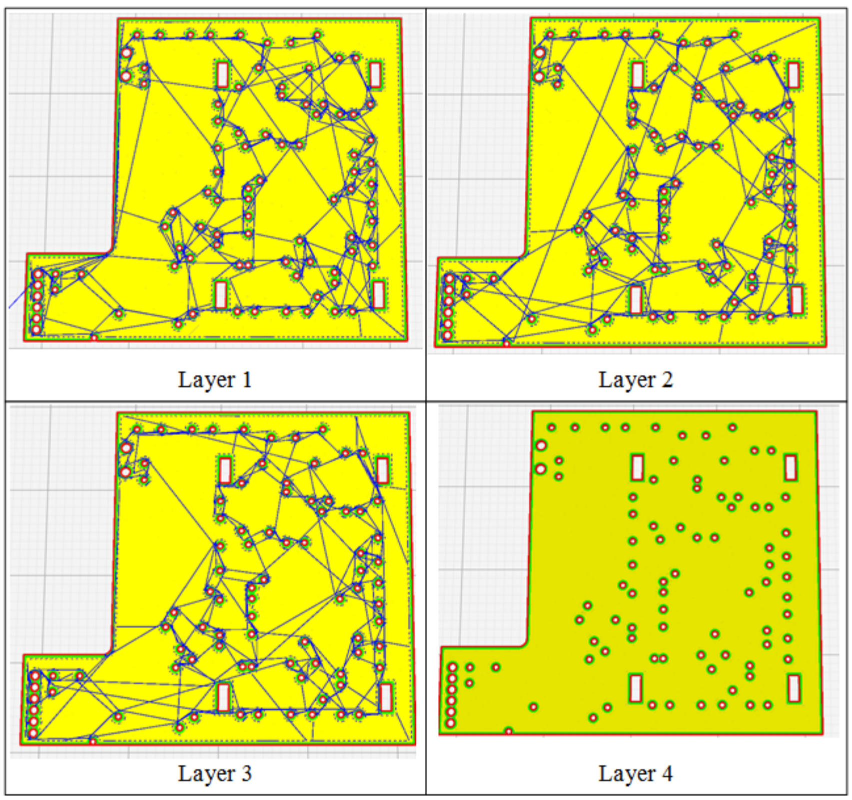

Fig. 6. Layers of the board with Cura®.

When the parameters and the orientation of the board were defined, the G code was generated. In this phase, the original sequence of the tool path was identified, and the coordinates of each slot were defined. As it has been shown in figures 6.a, 6.b and, 6.c, the trajectory of the tool was randomly creating crossings points and waste of time. The next lines present a part of the G code generate by Repetier® software, where is possible to identify the type of operation, the coordinates of X, Y, and Z, and the instruction for the extruder E.

```
LAYER:1
      M106 S63
      G0 F9000 X104.400 Y95.600 Z0.500
;TYPE:WALL-INNER
      G1 F2220 X104.400 Y104.400 E23.31466
      G1 X95.600 Y104.400 E23.60735
      G1 X95.600 Y95.600 E23.90004
      G1 X104.400 Y95.600 E24.19273
      G0 F9000 X104.800 Y95.200
;TYPE:WALL-OUTER
      G1 F1980 X104.800 Y104.800 E24.51203
      G1 X95.200 Y104.800 E24.83132
      G1 X95.200 Y95.200 E25.15062
      G1 X104.800 Y95.200 E25.46992
      G0 F9000 X104.230 Y95.739
```

Once the G code was ready, Table 2 was generated with the information of the coordinates for each initial node of the slots. It is important to highlight that the slots are closed geometries; in consequence, the start node is equal to the end node for each slot.

Table 2. Coordinates assigned for each start node of the slots in the board

	Slots type A			Slots type B			Slots type C	
	X	Y		X	Y		X	Y
A1	22.09	3.93	B1	1.47	1.39	C1	11.09	31.23
A2	22.09	30	B2	1.47	2.66	C2	11.09	34.11
A3	40.27	3.93	B3	1.47	3.94			
A4	40.27	30	B4	1.47	5.21			
			B5	1.47	6.48			
			B6	1.47	7.75			

				Slots type D				
	X	Y		X	Y		X	Y
D1	8.12	0.44	D28	40.11	11.08	D55	40.11	23.5
D2	17.75	1.99	D29	31.7	11.59	D56	24.51	24.32
D3	10.89	3.22	D30	22.08	12.32	D57	27.69	24.15
D4	19.36	3.16	D31	25.71	12.43	D58	22.08	25.77
D5	24.49	3.44	D32	37.71	12	D59	33.7	26.58
D6	26.49	3.44	D33	16	13.24	D60	36.5	26.58
D7	30.09	3.44	D34	20.17	13.24	D61	38.11	26.58
D8	32.5	3.44	D35	40.11	13.89	D62	22.08	27.8
D9	35.7	3.44	D36	25.71	14.46	D63	32.51	27.8
D10	37.71	3.44	D37	16.92	14.91	D64	34.5	27.8
D11	33.7	5.11	D38	40.11	15.88	D65	40.11	27.8
D12	3.46	5.94	D39	22.08	16.32	D66	29.64	28.88
D13	35.7	6.73	D40	25.71	16.49	D67	24.49	29.92
D14	3.46	7.75	D41	35.7	16.45	D68	29.68	29.92
D15	6.46	7.75	D42	20.98	17.3	D69	13.26	30.31

D16	31.3	7.54	D43	25.71	17.71	D70	13.26	32.25
D17	35.7	7.94	D44	37.71	17.67	D71	26.88	32.25
D18	17.21	8.67	D45	40.11	18.29	D72	32.89	32.25
D19	24.71	8.77	D46	27.07	18.67	D73	36.49	33.47
D20	25.71	8.77	D47	22.08	19.7	D74	38.5	33.47
D21	40.11	8.68	D48	38.11	19.7	D75	27.91	35.32
D22	30.09	9.16	D49	40.11	20.7	D76	30.72	35.32
D23	32.9	9.16	D50	38.11	21.72	D77	12.29	36.32
D24	19.01	9.59	D51	22.08	22.53	D78	15.09	36.32
D25	17.73	10.75	D52	25.31	22.72	D79	18.7	36.32
D26	37.71	10.38	D53	26.64	22.94	D80	21.1	36.32
D27	22.08	11.12	D54	31.7	22.94	D81	24.71	36.32
						D82	33.89	36.32

Using the original sequence (B2-B1-B3-B4-B5-B6D14-D12-D15-D3-D1-D2-D4-D25-D33-D37-D18-D24-D20-D19-A3-D10-D9-D38-D45-D49-D55-D21-D28-D35-D26-D32-D13-D17-D11-D8-D5-D6-D7-A1-D31-D22-D23-D29-D16-D48-D50-D44-D41-D65-A4-D61-D60-D64-D59-D63-D73-D74-D68-D66-D72-D76-D82-D81-D71-D75-D69-A2-D67-D70-C2-C1-D77-D78-D79-D80-D53-D54-D57-D52-D56-D58-D62-D51-D47-D42-D39-D34-D30-D27-D46-D40-D36). The extruder (Prusa I3 printing tool) needs to travel 610.18 mm. Figure 7 presents the route cover by the tool. 0,0 is the star node. The extruder first prints the shield (blue line) going from 0,0 to the right, then go up, then to the left, then go down, then go left and finally going to 0,0. After the shield, the tool travels to B2 to follow the sequence mentioned above. The time required by the extruder to print the slots was 254 seconds.

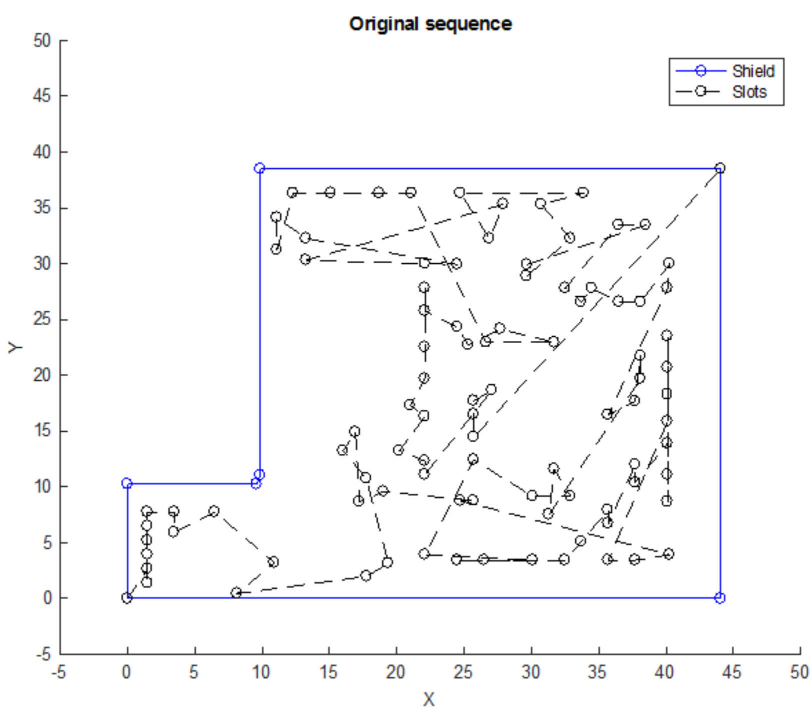

Fig. 7. Original Sequence followed by the printer to print layer 1.

To generate extruder travel alternatives, the K-NN algorithm was under the next:

O.f.: $M(s_o) = \min_s \Sigma_{(i,j)} c_{ij}$

Restrictions:
Equipment parameters defined for FFF Prusa I3 mentioned above.
Follow the sequence of slots printing by groups according to (A-B-C-D)
Every integer between 1 and n occurs at least once in t.

Under the constraint of printing slots by geometry, the algorithm generates the next sequence as a route. (A1-A2-A3-A4-B1-B2-B3-B4-B5-B6-C1-C2-D1-D2-D3-D4-D5-D6-D7-D8-D9-D10-D11-D12-D13-D14-D15-D16-D17-D18-D19-D20-D21-D22-D23-D24-D25-D26-D27-D28-D29-D30-D31-D32-D33-D34-D35-D36-D37-D38-D39-D40-D41-D42-D43-D44-D45-D46-D47-D48-D49-D50-D51-D52-D53-D54-D55-D56-D57-D58-D59-D60-D61-D62-D63-D64-D65-D66-D67-D68-D69-D70-D71-D72-D73-D74-D75-D76-D77-D78-D79-D80-D81-D82). In this case, the extruder had to cover 989.44 millimeters to visit each start node of the slots by layer. Figure 8 presents the route cover by the extruder. 0,0 is the star node. The extruder first generates the shield (blue line) going from 0,0 to the right, then go up, then to the left, then go down, then go left and finally going to 0,0. After the shield, the extruder travels to A1 to follow the sequence defined above.

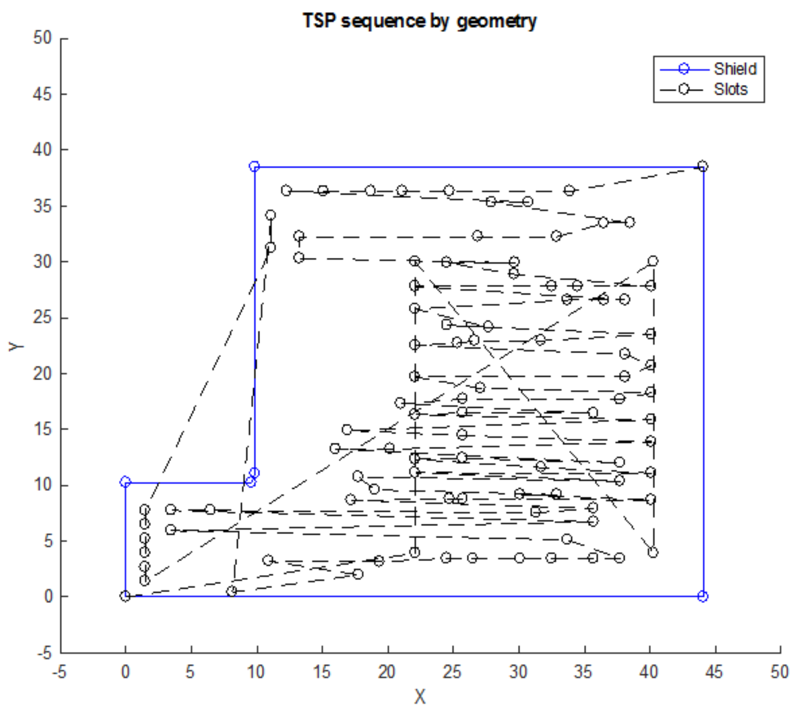

Fig. 8. Sequence by slots geometries, followed by the extruder to print layer 1.

O.f.: $M(s_o) = \min_s \Sigma_{(i,j)} c_{ij}$

Restrictions:
Equipment parameters defined for FFF Prusa I3 mentioned above.
Follow the sequence of slots printing by closest neighbor in the horizontal plane.
Every integer between 1 and n occurs at least once in t.

The sequence generated was (D1-B1-D2-B2-D3-D4-D5-D6-D7-D8-D9-D10-A1-A3-B3-D11-B4-D12-D13-B5-D16-D14-D15-D17-B6-D18-D19-D20-D21-D22-D23-D24-D26-D25-D28-D27-D29-D32-D30-D31-D33-D34-D35-D36-D37-D38-D39-D40-D41-D42-D43-D44-D45-D46-D47-D48-D49-D50-D51-D52-D53-D54-D55-D57-D56-D58-D59-D60-D61-D63-D64-D65-D62-D66-D67-D68-A2-A4-D69-C1-D71-D72-D70-D73-D74-C2-D75-D76-D77-D78-D79-D80-D81-D82). In this sequence, the extruder had to travel 1115.05 millimeters to visit each star node of the slots by layer. 0,0 is the star node. The extruder first generates the shield (blue line) going from 0,0 to the right, then go up, then to the left, then go down, then go left and finally going to 0,0. Then, extruder travels to D1 to cover the sequence mentioned above. Figure 9 presents the result of the extruder trajectory.

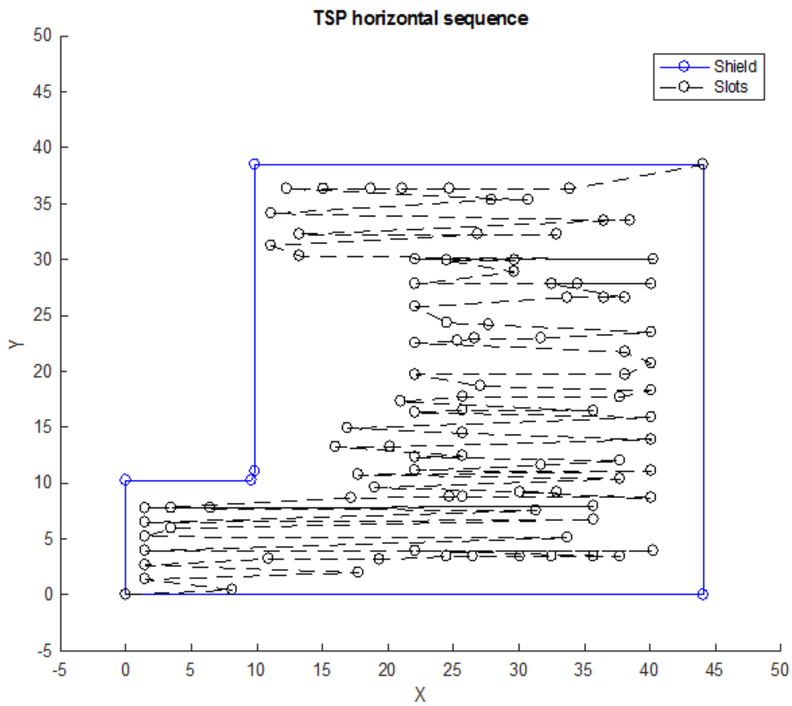

Fig. 9. TSP horizontal sequence, followed by the extruder to print layer 1.

O.f.: $M(s_o) = \min_s \Sigma_{(i,j)} c_{ij}$

Restrictions:

Equipment parameters defined for FFF Prusa I3 mentioned above.
Follow the sequence of slots printing by closest neighbor in the vertical plane.
Every integer between 1 and n occurs at least once in t.

The vertical route was developed, and the final sequence was defined by B1-B2-B3-B4-B5-B6-D14-D12-D15-D1-D3-C1-C2-D77-D70-D69-D78-D33-D37-D18-D2-D25-D79-D24-D4-D34-D42-D80-A2-D27-D30-D39-D47-D51-D58-D62-A1-D5-D19-D56-D67-D81-D52-D20-D31-D36-D40-D43-D6-D53-D71-D46-D57-D75-D68-D66-D76-D22-D7-D16-D54-D29-D63-D8-D23-D72-D82-D59-D11-D64-D41-D17-D13-D9-D60-D73-D44-D32-D26-D10-D48-D50-D61-D74-A4-D65-D55-D49-D45-D38-D35-D28-D21-A3. In this case, the extruder had to travel 786.65 by layer to fulfill its objective. The extruder first generates the shield (blue line) going from 0,0 to the right, then go up, then to the left, then go down, then go left and finally going to 0,0. Then, extruder travels to B1 to cover the sequence mentioned above.. Figure 10, presents the route cover by the tool.

O.f.: $M(s_o) = \min_s \Sigma_{(i,j)} c_{ij}$

Restrictions:

Equipment parameters defined for FFF Prusa I3 mentioned above.
Follow the sequence of slots printing by the closest neighbor.
Every integer between 1 and n occurs at least once in t.

Was possible to find an optimal sequence with the minimum time of travel that was defined by (B1-B2-B3-B4-B5-B6-D14-D12-D15-D3-D1-D2-D4-A1-D5-D6-D7-D8-D11-D9-D10-A3-D21-D28-D26-D32-D5-D38-D45-D49-D48-D50-D55-D61-D60-

D64-D59-D63-D66-D68-D71-D75-D76-D82-D73-D74-A4-D65-D72-D67-A2-D62-D58-D56-D52-D53-D57-D54-D46-D43-D40-D36-D31-D30-D27-D34-D25-D24-D18-D33-D37-D42-D39-D47-D51-D69-D70-C1-C2-D77-D78-D79-D80-D81-D41-D44-D29-D23-D22-D16-D17-D13-D20-D19), with this sequence the extruder had to travel 478.16 millimeters to visit each start node of the slots by layer. 0,0 is the star node. The extruder first generates the shield (blue line) going from 0,0 to the right, then go up, then to the left, then go down, then go left and finally going to 0,0. Then, extruder travels to B1 to cover the sequence mentioned above. Figure 11, exposes the route cover by the tool.

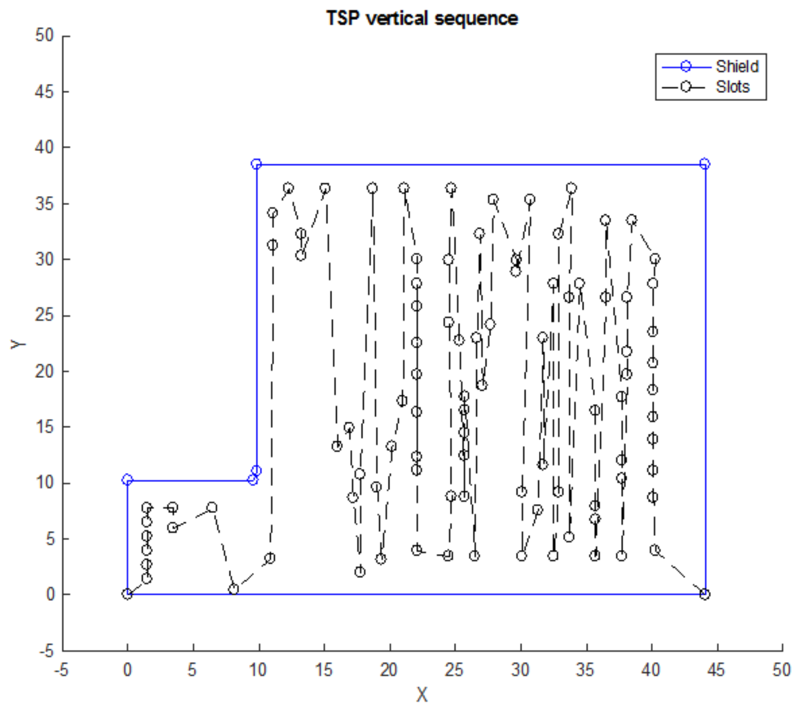

Fig. 10. TSP vertical sequence, followed by the extruder to print layer 1.

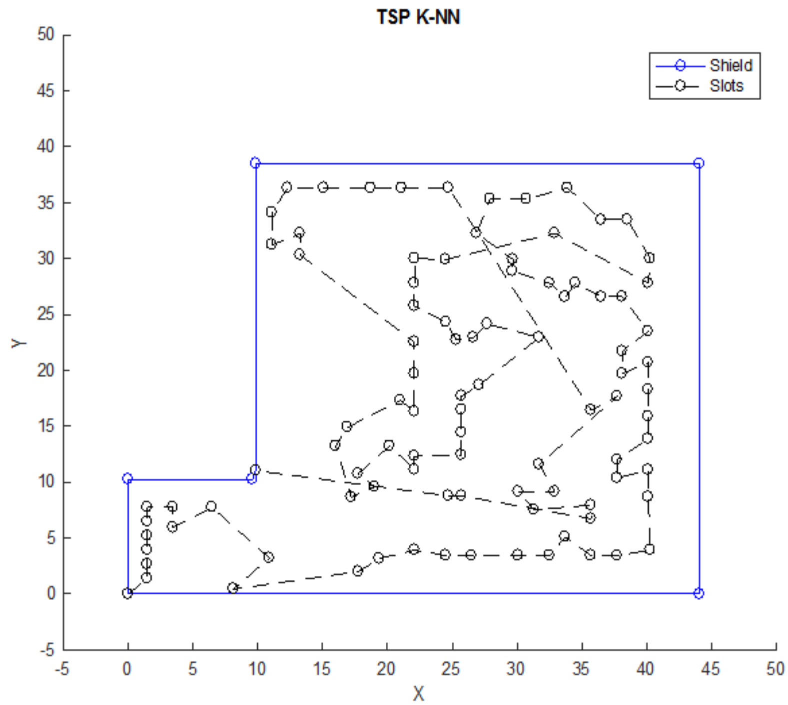

Fig. 11. TSP NNA sequence, followed by the extruder to print layer 1.

To compare the alternatives found, Table 2 was created considering the distance covered by the tool by layer, the time consumed by the extruder to cover the route, and the final time required for the extruder to generate the slots. In the case of the original sequence, an average distance was calculated because there was identified that the tool did not repeat the trajectory.

Table 2. Synthesis of the distances and times required by the extruder considering different alternatives of optimization.

Sequence	Distance traveled by layer (mm)	The time required by the tool to create the slots by layer (sec)	The final time required by the extruder to print the slots (sec)
Original sequence	610.18	5.08	254.00
TSP sequence by geometries	989.44	8.24	412.00
TSP horizontal sequence	1115.05	9.29	464.50
TSP vertical sequence	786.65	6.55	327.50
TSP-NNA	478.16	3.98	199.00

Table 2 demonstrates that print the slots consume 24.90% of the total time required to print the board. Considering that the conditions of the infield are the same for all the options, it is possible to assure that the process was optimized using the TSP-NNA, which consumed only 19.50% of the time to print the slots. In other words, printing the board with the original sequence consumed 17 minutes and printing the board with the TSP-NNA consumes 16 minutes, this is a reduction of 5.88% of the original time.

Once that the sequence was defined, the last step was to prepare the 3D printing equipment with the parameters mentioned above. Figure 11 presents an image of the PCB printed in FFF. This image presents the board with the four types of slots. It is possible to identify that the quality of the board is highly acceptable. The dimension of the slots is accurate and allow to insert the respective component to integrate the PCB.

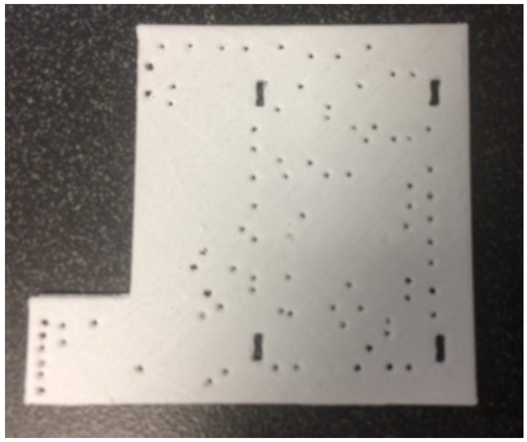

Fig. 11. Board printed with an optimized process.

5 Conclusions

The main goal of this research paper was to expose the use of the K-NN algorithm to reduce the time required by the extruder to cover the route that the FFF equipment consumes to print PCB slots. It had been followed two crucial directions: a) to reduce the extruder path length and b) minimization of the processing time. In this case, it was possible to use K-NN to reduce the final route to print the slots shield. As it has demonstrated, K-NN results appropriate even the algorithms used in the study begun with the same origin node, resulting in a reduction of the length needed by the extruder to finish the layer.

The nature of the FFF process is to follow a sequence generated by the pre-processing software. In this case, it has been demonstrated that the paths created by the pre-processing software are different between layers. The use of the TSP with K-NN allows replicating the optimized sequence layer by layer. This principle is a consequence of use origin node and end node, that changes their function layer by layer.

As it has shown in the last image (Figure 11), the board printed is adequate from the point of view of shapes definition and can be used to set a PCB. Finally, this research opens the opportunity to use other algorithms of optimization path that can be adapted to FFF, focused in the optimization of the length cover by the tool during the printing process, considering always satisfy the quality requirements and the feasibility of the element.

References

1 T. Thomas, S. R. Sherman, and R. S. Sawhney, “Application of lean manufacturing principles to improve a conceptual supply process,” *J. Manuf. Syst.*, vol. 46, pp. 1–12, 2018.

2 J. Corkery, M. Mikalsen, and K. Allan, *Corporate social responsibility: The good corporation*, First. Queenslabd: Bond University, 2017.

3 M. Kavanagh and R. Johnson, *Human resource information systems: Basics, applications, and future directions*, 4th ed. California, 2017.

4 I. C. Garretson, M. Mani, S. Leong, K. W. Lyons, and K. R. Haapala, “Terminology to support manufacturing process characterization and assessment for sustainable production,” *J. Clean. Prod.*, vol. 139, pp. 986–1000, 2016.

5 E. Lai, “U.S. Navy will rely on 1,000 3D printed parts by end of 2018 - 3D Printing Industry,” 2018. [Online]. Available: https://3dprintingindustry.com/news/u-s-navy-will-rely-1000-3d-printed-parts-end-2018-131910/?goal=0_695d5c73dc-11e515a067-64686269. [Accessed: 12-Apr-2018].

6 T. Lee, “27 charts that will change how you think about the American economy,” *New Money*, 2016. [Online].

Available: https://www.vox.com/new-money/2016/10/10/12933426/27-charts-changing-economy. [Accessed: 10-Apr-2019].
7 C. Weller, R. Kleer, and F. T. Piller, "Int . J . Production Economics Economic implications of 3D printing : Market structure models in light of additive manufacturing revisited," *Intern. J. Prod. Econ.*, vol. 164, pp. 43–56, 2015.
8 J. Beaman, D. Bourell, and D. Wallace, "Additive manufacturing and 3d Printing," *J. Manuf. Sci. Eng.*, no. Special Issue, 2014.
9 I. Campbell, D. Bourell, and I. Gibson, "Additive Manufacturing: Rapid Prototyping comes of age," *Rapid Prototyp. J.*, vol. 18, no. 4, pp. 255–258, 2012.
10 S. Mellor, L. Hao, and D. Zhang, "Additive manufacturing: A framework for implementation," *Int. J. Prod. Econ.*, vol. 149, pp. 194–201, 2014.
11 J. Gardan, "Additive manufacturing technologies: state of the art and trends," *Int. J. Prod. Res.* , vol. 54, no. 10, pp. 3118–3132, 2015.
12 B. Rylands *et al.*, "The adoption process and impact of additive manufacturing on manufacturing systems," *J. Manuf. Technol. Manag.*, vol. 27, no. 7, pp. 969–989, 2016.
13 G. Dong, G. Wijaya, Y. Tang, and Y. F. Zhao, "Optimizing process parameters of fused deposition modeling by Taguchi method for the fabrication of lattice structures," *Addit. Manuf.*, vol. 19, pp. 62–72, 2018.
14 T. Nancharaiah, D. R. Raju, and V. R. Raju, "An experimental investigation on surface quality and dimensional accuracy of FDM components," *Int. J. Emerg. Technol.*, vol. 1, no. 2, pp. 106–111, 2010.
15 A. K. Sood, R. K. Ohdar, and S. S. Mahapatra, "Improving dimensional accuracy of Fused Deposition Modelling processed part using grey Taguchi method," *Mater. Des.*, vol. 30, no. 10, pp. 4243–4252, 2009.
16 V. Kovan, G. Altan, and E. S. Topal, "Effect of layer thickness and print orientation on strength of 3D printed and adhesively bonded single lap joints," *J. Mech. Sci. Technol.*, vol. 31, no. 5, pp. 2197–2201, 2017.
17 K. Oettmeier and E. Hofmann, "Impact of additive manufacturing technology adoption on supply chain management processes and components," *J. Manuf. Technol. Manag.*, vol. 27, no. 7, pp. 944–968, 2016.
18 J. B. Jones, D. I. Wimpenny, and G. J. Gibbons, "Additive manufacturing under pressure," *Rapid Prototyp. J.*, vol. 21, no. 1, pp. 89–97, 2015.
19 C. O. Balderrama-Armendariz, E. MacDonald, D. Espalin, D. Cortes-Saenz, R. Wicker, and A. Maldonado-Macias, "Torsion analysis of the anisotropic behavior of FDM technology," *Int. J. Adv. Manuf. Technol.*, pp. 1–11, 2018.
20 M. Hinderdael *et al.*, "Proof of Concept of Integrated Load Measurement in 3D Printed Structures," *Sensors*, vol. 17, no. 2, p. 328, 2017.
21 S. Kumar, A. K. S. Choudhary, A. K. Singh, and A. K. Gupta, "A Comparison of Additive Manufacturing Technologies," *IIJIRST – Int. J. Innov. Res. Sci. Technol.*, vol. 3, no. 01, pp. 147–152, 2016.
22 Dddrop, "What are the advantages of FDM," 2018. [Online]. Available: https://www.dddrop.com/fdm-technology/. [Accessed: 10-Jun-2018].
23 M. Petch, "3D Printing Industry Jobs Board launches," *3D Printing Industry*, 2018. [Online]. Available: https://3dprintingindustry.com/news/3d-printing-industry-jobs-board-launches-130004/. [Accessed: 07-Mar-2018].
24 E. Soriano-Heras, F. Blaya-Haro, C. Molino, and J. M. de Agustín del Burgo, "Rapid prototyping prosthetic hand acting by a low-cost shape-memory-alloy actuator," *J. Artif. Organs*, vol. 0, no. 0, p. 0, 2018.
25 L. Chen, Y. He, Y. Yang, S. Niu, and H. Ren, "The research status and development trend of additive manufacturing technology.," *Int. J. Adv. Manuf. Technol.*, vol. 89, no. 9, pp. 3651–3660, 2016.
26 A. Boschetto, L. Bottini, and F. Veniali, "Finishing of Fused Deposition Modeling parts by CNC machining," *Robot. Comput. Integr. Manuf.*, vol. 41, pp. 92–101, 2016.
27 J. LaDou, "Printed circuit board industry," *Int. J. Hyg. Environ. Health*, vol. 209, no. 3, pp. 211–219, 2006.
28 A. Cabrera, "Ei barrenado de microagujeros en materiales no metálicos," *Ing. Mecánica*, vol. 1, pp. 69–75, 2001.
29 K. Altinkemer, B. Kazaz, M. Köksalan, and H. Moskowitz, "Optimization of printed circuit board manufacturing: Integrated modeling and algorithms," *Eur. J. Oper. Res.*, vol. 124, no. 2, pp. 409–421, 2000.
30 M. Ancău, "The processing time optimization of printed circuit board," *Circuit World*, vol. 35, no. 3, pp. 21–28, 2009.
31 A. Canal Marques, J. M. Cabrera, and C. De Fraga Malfatti, "Printed circuit boards: A review on the perspective of sustainability," *J. Environ. Manage.*, vol. 131, pp. 298–306, 2013.
32 Electrosoft Ingeniería, "Basic PCB concepts," *PCB*, 2010. [Online]. Available: http://www.pcb.electrosoft.cl/04-articulos-circuitos-impresos-desarrollo-sistemas/01-conceptos-circuitos-impresos/conceptos-circuitos-impresos-pcb.html. [Accessed: 18-Apr-2019].
33 A. Vidal, "Algoritmos Heurísticos de Optimización," Santiago de Compostela, 2013.
34 G. Croes, "A Method for Solving Traveling-Salesman Problems," *Oper. Res.*, 1958.
35 N. S. Altman, "An introduction to kernel and nearest-neighbor nonparametric regression," *Am. Stat.*, vol. 46, no. 3, pp. 175–185, 1992.
36 Dassault Systèmes SolidWorks Corporation, "SOLIDWORKS." 2017.
37 Ultimaker B.V., "Ultimaker Cura Software." Geldermalsen, 2018.

38 Hot-World GmbH & Co. KG, "Repetier." USA, 2018.
39 MathWorks, "MATLAB." Standford, 2013.
40 J. Kirk, "Traveling Salesman Problem - Genetic Algorithm." Matlab, 2000.